

PARTICLE PRODUCTION IN JETS AND IN COLLISIONS BETWEEN HADRONS AND/OR NUCLEI*

BY G. GUSTAFSON

Department of Theoretical Physics, University of Lund**

(Received November 6, 1986)

A new model for low- p_{\perp} hadron-hadron, hadron-nucleus and nucleus-nucleus collisions is presented together with a review of the Lund model for hadronization in quark and gluon jets.

PACS numbers: 13.85.Hd

1. Introduction

In these talks I first want to briefly discuss the Lund model for hadronization in quark and gluon jets (for an extensive review see Ref. [1]) and then present a new model for low- p_{\perp} hadron-hadron, hadron-nucleus and nucleus-nucleus collisions [2]. This model has the same features with respect to the quantum number flows in the fragmentation regions as our earlier low- p_{\perp} model. However, it has a more satisfying colour field structure, which is directly generalizable to hadron-nucleus and nucleus-nucleus collisions. It also gives a good description of the central rapidity plateau, which implies that it can be used in a wider energy region up to the top ISR energies. In its present form it does not include hard parton-parton interaction and thus it does not contain high- p_{\perp} jet or Drell-Yan production.

The model is based on "conventional colour dynamics" and thus does not contain any effects of new phenomena such as a phase transition to a quark-gluon plasma. We believe that when analyzing new data from high energy nucleus-nucleus collisions, it is very valuable to be able to compare with such a conventional model in order to judge possible signals for new physics. Such a comparison is facilitated by a Monte Carlo simulation program [3] which is available for the interested investigator.

* Presented at the XXVI Cracow School of Theoretical Physics, Zakopane, Poland, June 1-13, 1986.

** Address: Department of Theoretical Physics, University of Lund, Sölvegatan 14A, S-223 62 Lund, Sweden.

2. Hadronization in quark and gluon jets

Quark jets

At moderate energies hadron production is dominated by the longitudinal phase space, i.e. limited transverse momenta and a multiplicity which grows like $\ln(s)$. These properties are expected from hadronization in a homogeneous colour force field. A linear electric field is invariant under longitudinal Lorentz transformations. When the energy in the field is transferred into hadrons we expect a plateau in rapidity, and also a potential which is linear in the distance, r , and an area law for Wilson loop integrals.

The motion of a quark and an antiquark, which are connected by a linear potential, $V = \kappa r$, and move in one space dimension, is depicted in Fig. 1. The situation for a high energy $q\bar{q}$ system is shown in Fig. 2. When the particles move apart much energy is stored in the field, and from this energy new $q\bar{q}$ pairs are produced, which combine to the observable mesons in the final state. All the production points have space-like distances to each other, and are therefore causally disconnected. Thus no production point in more funda-

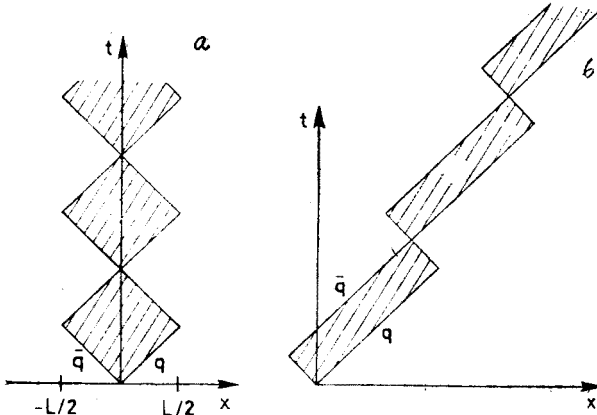


Fig. 1. a) The motion of q and \bar{q} in the cm frame. The hatched areas show where the field is non-vanishing, b) The same motion in a Lorentz frame boosted relative to the cm frame

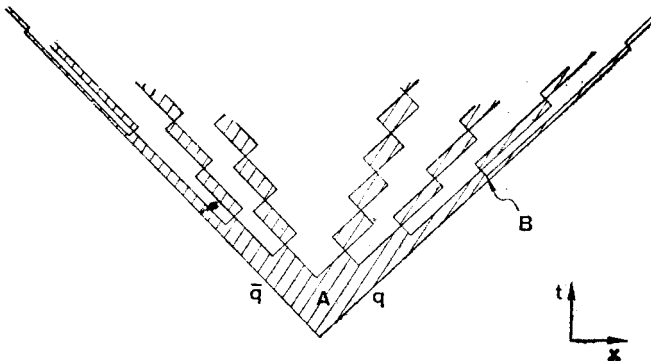


Fig. 2. The final picture when q and \bar{q} move with large energies in opposite directions. The field has broken at many places by the production of new $q\bar{q}$ pairs

mental than the other; which production occurs first in time depends on the Lorentz frame used. We start by studying the meson furthest to the right in Fig. 2, i.e. the one which contains the original quark q plus the antiquark \bar{q}_1 produced at the point B in Fig. 2. This meson is called first rank, but it is not necessarily the fastest one. We assume that for large total energies the energy of this first rank meson is given by a probability distribution

$$\frac{dP}{dz} \equiv f(z), \quad z \equiv (E+P)_{\text{meson}}/(E+P)_{\text{total}}. \quad (1)$$

The remaining system is now very similar. The leading quark q is replaced by q_1 and the total cms energy is reduced. The fraction of the remaining energy taken by the next (second rank) meson should also be given by the same probability distribution $f(z)$. This leads to an integral equation. However, the existence of many types of mesons and resonances implies that we get a set of coupled equations, which are most easily solved by Monte Carlo techniques.

However, the mesonic final state in Fig. 2 could equally well be generated starting from the meson furthest to the left (the one containing the original antiquark \bar{q}). In this way the same result should be obtained and this condition gives severe restrictions on the probability distribution $f(z)$, which has to be of the form [4]

$$f(z) = N \frac{(1-z)^a}{z} \exp(-bm^2/z). \quad (2)$$

Here m is the meson mass and the three constants N , a and b are related by a normalization condition, so that there are two free parameters. The result in Eq. (2) also follows from the assumption that any $q\bar{q}$ -pair creation splits the total system in two pieces which decay further independently of each other.

Our result has a very nice interpretation in the following way. From Eq. (2) it is possible to calculate the probability to obtain a definite final state with n mesons with momenta p_i ($i = 1, \dots, n$). This probability is given by the following expression

$$\text{Prob} \propto \prod_{i=1}^n [Nd^2 p_i \delta(p_i^2 - m^2)] \delta(\sum p_i - P_{\text{tot}}) \exp(-bA), \quad (3)$$

where A is the space-time area in Fig. 2, spanned by the field before it breaks into mesons. This expression has the form of a phase space factor times the exponent of a kind of effective action bA . This action can be interpreted as a "colour coherence area" in space-time, resembling a Wilson loop integral.

In Eq. (3) it is assumed that all mesons have the same mass m . This is however no necessary restriction. With different hadron masses we note that the particles will be ordered in rapidity rather than in momentum. In particular the fragmentation distribution for a charm quark into a charm meson becomes rather hard, in good agreement with experiments [1].

Gluon jets

Up to now we have studied fragmentation in a 1+1 dimensional world. In 3+1 dimensions Lorentz covariance and causality imply that the potential cannot depend only on the distance between a quark and an antiquark. If the quark gets a kick, it takes some time before the antiquark can notice anything (cf. Fig. 3). If the force field is compressed to a linear structure, this structure has to bend and also to carry momentum when it moves transversely. This must correspond to extra degrees of freedom. The state is not fully described by the positions of the colour charges of the quark and the antiquark; also the

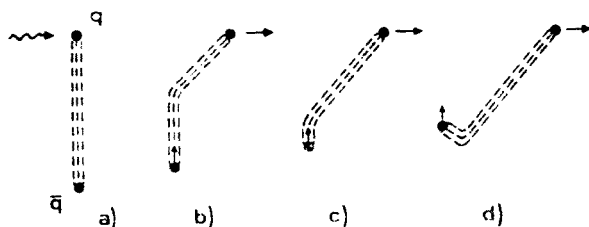


Fig. 3. The motion of the colour field when the quark gets a kick illustrates that the antiquark cannot notice anything until it is reached by the disturbance of the field which moves with the velocity of light

string configuration has to be specified. Thus it must be possible to make excitations on the field. If we neglect the transverse dimension and study a very thin tube with a strong electric field, or a vortex line, then this tube or vortex line will move according to the dynamics of the massless relativistic string.

The energy and momentum of such a string can easily be calculated from their relativistic transformation properties. Thus a string element with length dl and transverse velocity v_{\perp} has energy and momentum given by the relations

$$dE = \frac{\kappa dl}{\sqrt{1-v_{\perp}^2}}; \quad dP_{\perp} = dE \cdot v_{\perp}, \quad (4)$$

where κ is the string tension at rest. For a moving string the tension is $\kappa \sqrt{1-v_{\perp}^2}$.

At higher energies we know that there can be gluon radiation in e.g. an e^+e^- -annihilation event, $e^+e^- \rightarrow q\bar{q}g$. In the Lund model we assume that the gluon behaves as a transverse excitation, or a kink, on the stringlike field [5]. Thus the string is stretched from the quark via the gluon to the antiquark (see Fig. 4). The string breaks into hadrons in the same way as described above, and thus gluon fragmentation is determined from the quark fragmentation. The transverse velocity of the string (see Fig. 4) gives extra momentum to the hadrons, which thus are produced around two hyperbolae in momentum space (cf. Fig. 5a). In this way there will be a depletion of particles in the angular region opposite to the gluon jet, and this asymmetry is clearly observed in the experiments [6].

In the Lund model there is only one type of string, which has a colour triplet and an antitriplet at its endpoints. One could also imagine that the gluon is attached to a colour octet string, which at a junction is split into two colour triplet strings [7]. However, if the tension in the octet string is twice the triplet string tension or larger, then the octet string

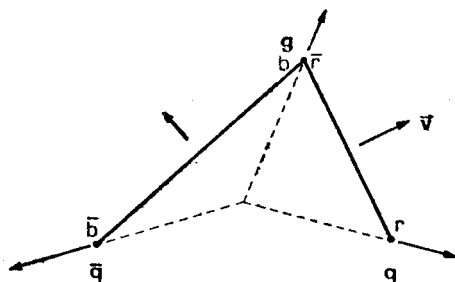


Fig. 4. In the Lund model the colour field is stretched from the quark via the gluon to the antiquark, i.e. in the example from red to antired and from blue to antiblue

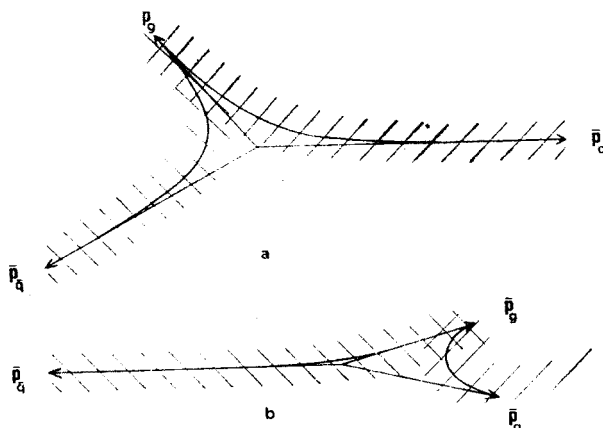


Fig. 5 a) The string in Fig. 4 has a transverse velocity which gives extra momentum to the hadrons. Therefore these are produced around two hyperbolae in momentum space, b) A quark and an almost collinear gluon produce hadrons in a way similar to a single quark. Thus e.g. one hadron can take more energy than any of the partons

shrinks to zero length. As lattice calculations give such a large octet string tension, this gives further support to the Lund gluon model [8].

A similar asymmetry in the produced hadrons is also obtained in perturbative jet cascade calculations, if certain interference effects from soft gluons are included [9]. Parton clusters are produced preferentially between the quark and the gluon and between the gluon and the antiquark. However, the angular distribution of $B\bar{B}$ pairs produced in e^+e^- -annihilation shows that when the clusters decay they know the direction to their neighbours. Thus the clusters behave as links in a chain (i.e. like a string).

Infrared stability

A very essential feature of the string model is that it provides a natural cut off for the divergencies connected to soft and collinear gluons. For a collinear gluon the energy in the field between the gluon and the quark (or antiquark) is so small that the string cannot break here. The first break will be on the other side of the gluon kink, so that both the quark and the kink go into the same first rank hadron. Thus the hadron can take more energy

than any of the partons and the gluon and the quark will look just as a single quark jet (cf Fig. 5b).

For a state with many gluons we get a string with many kinks. There is a direct correspondence between a parton state and a string state. For the parton state we then have to specify not only the momenta but also the colour ordering of the gluons. Now the string state is not much changed if one low mass gluon is split into two. When the string fragments into hadrons, this implies a finite resolution power on the string or parton state, given by the hadronic mass scale. In this way the string model is *infrared stable*. There is a smooth transition between 3-jet and 2-jet events, between 4- and 3-jets etc.

This implies an effective cut off for soft and collinear gluons which can be most conveniently studied in the energy-energy correlations. At small angles this correlation is very sensitive to the cut off for the singularities, and the experimental data are very well reproduced by the string model when the cut off is set so low that essentially all events are treated as 3- or 4-jet events [10]. In this case many events with collinear gluons look almost like 2-jet events, and the effective cut off given by the string fragmentation gives just the observed result.

Υ -decay

Also for the decay of heavy quarkonia the Lund model gives a good description of the data. For the decay $\Upsilon \rightarrow 3g$ the string forms a closed triangular loop. The model does well reproduce the multiplicity and particle composition of the final state [11]. In case the gluons were connected by colour octet fields, we would expect this to break by gluon-gluon production, and thus we would expect to produce glueballs or states which mix with glueballs. Thus Υ -decay gives further support to the picture with only one type of string (the colour triplet string).

A probability measure on parton states

In the above discussion of e.g. e^+e^- -annihilation events, it is assumed that the reaction can be divided in two phases. First there is a perturbative phase in which there is a high energy concentration and where gluons may be radiated. Second, there is a nonperturbative phase in which a confining colour force field is stretched between the coloured partons. Here the energy concentration is low, and new $q\bar{q}$ -pairs are produced which combine to the final state hadrons.

However, we have also made an attempt to join the two phases. A possible interpretation of gluon radiation might be that at large energy many states are possible, and the phase space for a smooth straight string (corresponding to a state with no extra gluons) is relatively small. We have proposed a probability measure [12], which has the form of a phase space factor times the exponent of an effective action

$$\text{Prob} \sim \text{Phase space} \times \exp(-S_{\text{eff}}), \quad (5)$$

where S_{eff} is a characteristic area in Minkowski space spanned by the string before it breaks into pieces. The form is thus very similar to the hadronization probability in Eq. (3). This probability measure reproduces essential features of perturbative QCD. It is however

everywhere finite and it interpolates smoothly between the pole expressions of perturbative QCD. In particular it also reproduces the angular cut off in QCD cascades discussed by Mueller, Marchesini, Webber et al. [9].

Summary

The discussion in this Section can be summarized in the following points:

- 1) The confining force field seems to behave like a string or a vortex line in a superconductor.
- 2) Gluons behave like transverse excitations or kinks on the string.
- 3) This string picture is infrared stable.
- 4) The fragmentation of the string is determined by $(\text{phase space}) \times \exp(-S)$ where the effective action S is given by an area in space-time resembling a Wilson loop integral.
- 5) We have proposed a probability measure on string states, which also has the form $(\text{phase space}) \times \exp(-S_{\text{eff}})$, where again S_{eff} is an area in Minkowski space. This measure reproduces essential features of perturbative QCD.

3. A model for collisions between hadrons and/or nuclei

Some years ago we noticed a large similarity between hadron fragmentation and quark fragmentation [13]. Thus, e.g. the fragmentation of a π^+ in an hadronic collision is very similar to the average of u - and \bar{d} -fragmentation as observed in DIS or e^+e^- -annihilation. Also the fragmentation of a proton looks the same in a hadronic collision and in a DIS event. In the latter case a diquark system is left in the proton fragmentation region, and thus it seems as if also in hadronic collisions we have hadronization of a diquark system in the proton fragmentation region.

In e.g. a πp scattering event it seems as if we have a string which in the pion end is stretched out by one of the pion valence quarks and in the proton end by a diquark system. What do we have in the central region? The total multiplicity is approximately the same as in a DIS event. This would be the case if the two fragmentation regions were connected just by a single string, and a Monte Carlo simulation program was constructed on this idea. This program worked very well in reproducing inclusive particle spectra up to SPS-FNAL energies.

However, this model has a set of problems:

- 1) The multiplicity fluctuations in the model are too small.
- 2) The rise of the central plateau in the ISR region is not reproduced.
- 3) The colour structure is not consistent.
- 4) There is no smooth transition to high- p_{\perp} events.
- 5) There is no simple generalization to nucleus collisions.

The problem in point 3 arises because a string has a direction, defined e.g. as going from 3 to $\bar{3}$. In e.g. a pp collision we have a diquark, which is $\bar{3}$, in each end, and therefore the string has to change direction at some point.

For problem 4 we note that in a collision with a hard gluon-gluon scattering the hadron remnants are left in colour octet states. These are pulled back by two strings, which connect

them to the scattered gluons and to each other. When the gluon-gluon scattering becomes soft, the system goes over into two strings stretched between the hadron remnants. The cross-section for this scattering is divergent and the picture is not infrared stable. Soft gluon interactions give qualitative changes in the state and the result becomes cut-off dependent.

A new model

To cure these problems we have proposed a new model [2]. This model is based on the assumption that the colour field behaves like a vortex line in a superconducting vacuum. Such a vortex line in a type II superconductor consists of a thin core, which is kept together by currents circulating around it, and surrounded by a more extended magnetic field, which at large distances is exponentially damped. The field of such a vortex line is the same as that of a chain of dipoles lined up along the vortex. As long as the bending radius of the structure is larger than the core-radius it moves like a massless relativistic string. Thus two vortex lines can interact when their extended fields overlap, but their subsequent motion is determined by the dynamics of the string.

As a model for the interaction between two hadrons we assume that the dipole links in the vortex lines scatter incoherently like (almost) massless partons. (The number of links, partons, in a hadron is obviously determined by the resolution power, related to the energy available in the collision). The partons will exchange momentum but we assume that in soft low- p_T collisions there is no colour exchange; such an exchange could always be compensated by the further exchange of soft gluons. (In other cases like weak decays it has shown to be very easy to exchange soft gluons.) In this respect the model is infrared stable, as soft gluons are not allowed to exchange colour charge and thereby change the qualitative structure of the colour field.

Momentum transfer

It turns out that the total momentum transfer is the important quantity. For the transverse components we assume, from our incoherent parton picture, a stochastic behaviour similar to a Brownian motion in the transverse plane. This assumption implies a rather small total transverse momentum exchange. However, for the longitudinal components the contributions from many soft parton-parton collisions add up and may lead to sizeable momentum transfers.

Introducing a lightcone notation along the direction of approach (and transverse to that direction two-dimensional momentum vectors with index \perp) we use unprimed and primed parameters for the forward and backward moving initial hadrons:

$$\begin{aligned} P^i &= \left(P_+, \frac{m^2}{P_+}, \vec{0}_\perp \right), \\ P'^i &= \left(\frac{m'^2}{P'_-}, P'_-, \vec{0}_\perp \right), \end{aligned} \tag{6}$$

with P_+ and P'_- large compared to the hadron masses m and m' .

The scattering between a pair of partons with negligible masses and fractional lightcone energy-momenta x and x' will mean an exchange of transverse momentum \vec{k}_\perp . For small values of k_\perp such a collision has a relatively small effect on the "forward" light cone components, but the final state partons will also obtain "opposite" lightcone components given by

$$\delta k_- = \frac{k_\perp^2}{xP_+}, \quad \delta k'_+ = \frac{k_\perp^2}{x'P'_-}. \quad (7)$$

From these relations we note that also with limited k_\perp -values many collisions with small x and x' may add up to sizable total longitudinal momentum transfers

$$Q_- = \sum \delta k_{-j}, \quad Q_+ = \sum \delta k'_{+j}. \quad (8)$$

Using Feynman's wee parton spectrum, dx/x , we obtain from these relations for large values of Q_- and Q_+ roughly the scaling distribution

$$\text{Prob} \sim \frac{dQ_-}{Q_-} \cdot \frac{dQ_+}{Q_+}. \quad (9)$$

As a result of the collision we obtain two excited systems with the following momenta

$$P^f = \left(P_+ - Q_+, \frac{m^2}{P_+} + Q_-, \bar{0}_\perp \right) \approx (P_+ - P'^f_+, P^f_-, \bar{0}_\perp),$$

$$P'^f = \left(\frac{m'^2}{P'_-} + Q_+, P'_- - Q_-, \bar{0}_\perp \right) \approx (P'^f_+, P'_- - P^f_-, \bar{0}_\perp), \quad (10)$$

where the "backward" components P^f_- and P'^f_+ are usually large compared to the initial backward momenta m^2/P_+ and m'^2/P_- but small compared to the initial forward momenta P'_- and P_+ .

For small values of Q_- and Q_+ there has to be a cut off for the distribution in Eq. (9). We assume that this cut off is set by the hadronic mass scale in such a way that we get a scaling probability distribution in $P^f_- = Q_- + m^2/P_+$ and $P'^f_+ = Q_+ + m'^2/P'_-$.

$$\text{Prob} \sim \frac{dP^f_-}{P^f_-} \cdot \frac{dP'^f_+}{P'^f_+}. \quad (11)$$

From Eq. (10) we see that this also implies a scaling distribution in the masses of the excited systems $M^2 = (P^f)^2$ and $M'^2 = (P'^f)^2$

$$\text{Prob} \sim \frac{dM^2}{M^2} \cdot \frac{dM'^2}{M'^2} \quad (12)$$

(The motivation for this cut off is essentially given by the good results obtained.)

Fragmentation

As mentioned above the excited systems move according to the dynamics of a relativistic string. It turns out that if the momentum transfer is reasonably smoothly distributed over the hadron string, the string will be stretched out in the longitudinal direction in essentially the same way as the stringlike colour field in an e^+e^- -annihilation or a deep inelastic scattering event, see Fig. 6. Only if the momentum transfer is localized in the middle of the string, the string is stretched in a folded manner. (The centre will be pulled backwards and the two ends will point forwards.)

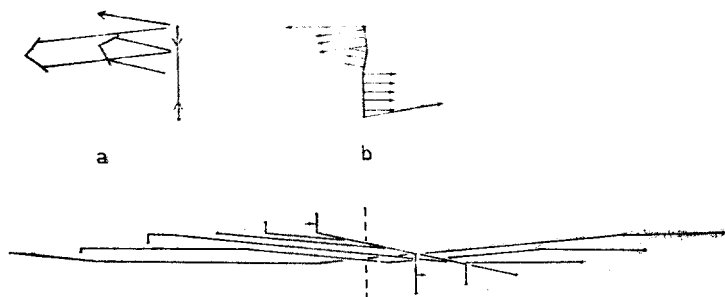


Fig. 6. The motion of a string (hadron) after the transfer of a large momentum. The string is stretched out and can fragment in a way similar to an e^+e^- annihilation or a DIS event; a) shows the momentum transfer in the original hadron cms; b) shows the excited system in its new cms after the hit; c) illustrates the subsequent motion at six different times until the string is fully stretched out

We assume that such well localized momentum transfers correspond to hard scattering events and that they can be neglected in the same energy region where high- p_{\perp} parton-parton scattering can be neglected for minimum bias events. According to calculations based on perturbative QCD [14] the probability for a hard scattering with $p_{\perp} > 2 \text{ GeV}/c$ is 6% at $\sqrt{s} = 63 \text{ GeV}$ and 40% at $\sqrt{s} = 540 \text{ GeV}$. Thus it ought to be possible to neglect hard scatterings up to the top ISR energies but not beyond. Thus in this energy region we assume that the excited systems fragment along the beam direction just like e^+e^- -annihilation or deep inelastic scattering events, but with the initial hadron valence flavours at the end points.

If we summarize our discussion we see that the interaction produces two longitudinally excited systems with momenta and masses given by Eqs (10)–(12). When these systems fragment they will produce particles in the two rapidity ranges

$$\begin{aligned}
 -\ln \left[\frac{P_-^f}{m_0} \right] &\lesssim y \lesssim \ln \left[\frac{P_+ - P_+^{f'}}{m_0} \right] \approx \ln \left[\frac{P_+}{m_0} \right], \\
 -\ln \left[\frac{P_-^{f'}}{m_0} \right] &\approx -\ln \left[\frac{P_- - P_-^f}{m_0} \right] \lesssim y \lesssim \ln \left[\frac{P_+^{f'}}{m_0} \right].
 \end{aligned} \tag{13}$$

Here m_0 is a typical hadron transverse mass. As P_-^f is logarithmically distributed, we see that the first system fills the rapidity range between the maximum rapidity value and a point

which is evenly distributed between the maximum and minimum values. The other system will naturally in the same way produce particles in the backward direction. On the average the two strings produce particles in a way very similar to the production from one single string. Thus the results for inclusive spectra are similar to those of the earlier one string model. However, there will be a noticeable change in the multiplicity distribution, because there are sometimes two short strings and sometimes two long strings, which are partly overlapping (in rapidity space). This gives much larger multiplicity fluctuations than a single string even if the average particle production is the same. Actually, the fluctuations turn out to be in very good agreement with data, as seen in Fig. 7.

At ISR energies the masses M and M' of the excited hadrons can be rather large, and we note that in the corresponding e^+e^- -annihilation and deep inelastic scattering processes it is possible to radiate off gluons, which show up as three-jet systems. According to perturbative QCD gluon emission is described by the dipole radiation formula

$$\frac{4}{3} \cdot \frac{\alpha_s}{\pi} \cdot \frac{dk_{\perp}^2}{k_{\perp}^2} dy \quad (14)$$

both in e^+e^- -annihilation and in deep inelastic scattering. The essential variable is the available energy, W , and there is in the case of deep inelastic scattering only a minor dependence on the variable Q^2 . When colour charges are rapidly separated they radiate gluons, and we expect gluons to be emitted in the same way in the excited systems discussed

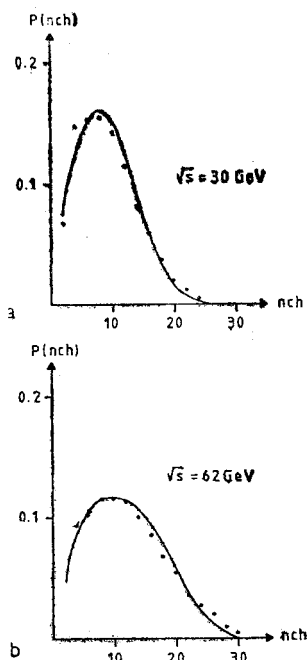


Fig. 7. Charged particle multiplicity distributions for pp collisions a) $\sqrt{s} = 30$ GeV and b) $\sqrt{s} = 62$ GeV. The lines are the model predictions and the data points are from Ref. [17]

here. In the Lund fragmentation model gluon emission corresponds to a bent string. Thus, whenever the endpoints of a string are violently pulled apart, the string has a tendency to bend or vibrate.

The phenomenological consequences of this gluon emission is an increase in multiplicity and in transverse momentum. At SPS energies there are only few gluons with energies large enough to give visible jets. Thus the multiplicity is essentially unchanged, but the p_{\perp} -distribution gets a larger tail and obtains an exponential shape rather than a Gaussian, as obtained from the fragmentation of a straight string. However, at ISR energies the increase in multiplicity will cause a rising central plateau, together with increasing $\langle p_{\perp} \rangle$. Some comparisons with data are shown in Figs 8–11.

The model discussed here has some features in common with the DTU-model [15] but there is a set of differences. In the DTU-model there is a recoupling so that two strings emerge stretched between valence constituents from the two different original hadrons. There are also a varying number of string fields stretched between sea constituents. In that model the rising central plateau is caused by an increased overlap between the two “main”

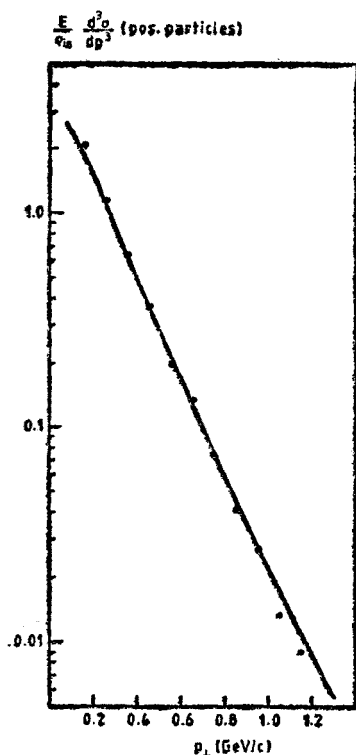


Fig. 8

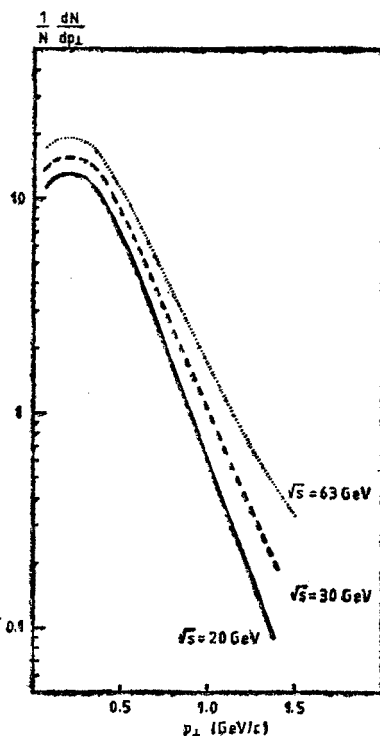


Fig. 9

Fig. 8. p_{\perp} distributions for positive particles in pp collisions at $\sqrt{s} = 53$ GeV. Line: The model predictions. Dots: Data from Ref. [18]

Fig. 9. Charged particle transverse momentum distribution $(1/N) (dN/dp_{\perp})$ for pp collisions at the energies $\sqrt{s} = 20$ GeV, 30 GeV and 62 GeV

strings and an increased number of “smaller” strings. In our model there is equally often a gap in rapidity space as an overlap between the two systems, and the increase in the centre is caused by increased gluon radiation at higher energies. The central plateau and $\langle p_{\perp} \rangle$ rise in a correlated way.

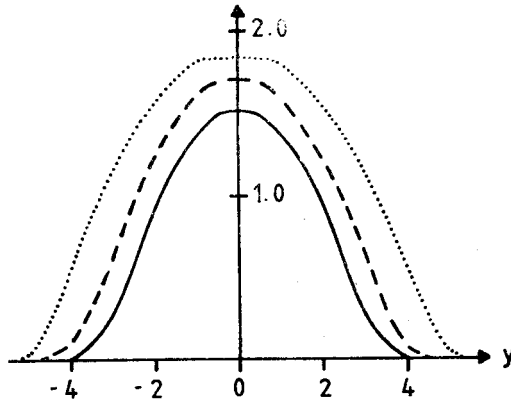


Fig. 10. Charged particle rapidity distributions for pp collisions. Full curve: $\sqrt{s} = 20$ GeV, dashed curve: $\sqrt{s} = 30$ GeV and dotted curve $\sqrt{s} = 62$ GeV

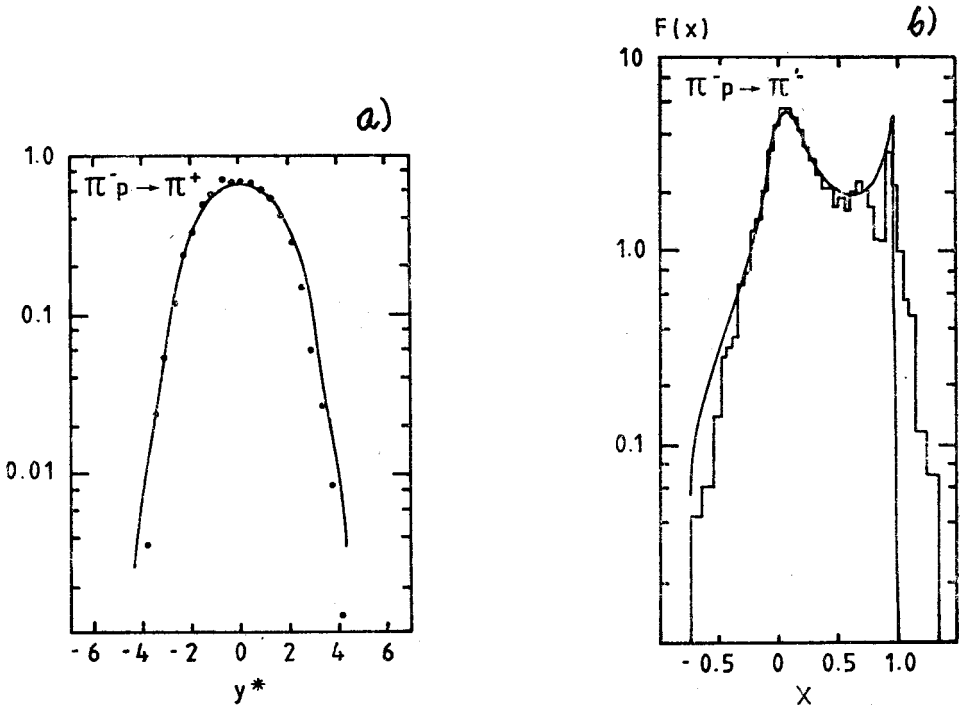


Fig. 11 a) Rapidity distribution for $\pi^- p \rightarrow \pi^+$ at 100 GeV. Line: The model predictions. Dots: Data from [19], b) x_F distribution for $\pi^- p \rightarrow \pi^-$ at 100 GeV. $F(x) = \int (2E/\pi\sqrt{s}) (d^2\sigma/dx dp_{\perp}^2) dp_{\perp}^2$. Line: The model predictions. Data from Ref. [19]

Diffraction

From the mass distribution in Eq. (12) we see that events where M or M' take on their minimal values, i.e. m or m' , look exactly like single diffractive excitation events. Experimentally diffractively excited systems are also known to fragment along the beam axis in accordance with the assumptions above [16]. Obviously the mass M cannot take on continuous values above the original hadron mass m . In case of an incoming proton, events generated by the computer simulation program with $m_p < M < 1.2$ GeV are adjusted so that M equals the initial mass m_p . With this recipe the probability for such events corresponds to the experimentally observed cross-section for single diffractive excitation. Thus diffractive excitation should not be removed from the data before comparing with the Monte Carlo generated results (cf. Fig. 11b).

Hadron-nucleus and nucleus-nucleus collisions

This hadron-hadron scattering model can be straightforwardly generalized into a model for hadron-nucleus and nucleus-nucleus collisions. For a hadron-nucleus collision the hadron encounters a set of collisions with nucleons in the nucleus. After the first collision the excited beam hadron has no time to fragment before the next collision. We assume that the different subcollisions can be treated incoherently. In each subcollision the impinging hadron and its collision partner will suffer longitudinal energy-momentum transfers, Q_+ and Q_- like the ones discussed above. Thus with v subcollisions we will end up with $v+1$ excited systems with light-cone components

$$\left(P_+ - \sum Q_{+n}, \frac{m^2}{P_+} + \sum Q_{-n} \right), \quad \left(\frac{m'^2}{P'_{-n}} + Q_{+n}, P'_{-n} - Q_{-n} \right), \quad n = 1, \dots, v. \quad (15)$$

It is assumed that in each of the subcollisions the resulting momenta are given by the same probability distribution in P_-^f and P_+^f (Eq. (11)). The only difference is that in the subsequent collisions the kinematic limits are different; the 'backward' momentum P_-^f is assumed to increase in each subcollision, and thus the lower limit is enhanced for the subsequent collisions. The lower energy in the subsequent collisions also decrease the maximum value of P_+^f for the target nucleons.

This picture can evidently be directly generalized also to nucleus-nucleus collisions although there is an extensive bookkeeping in order to keep track of the many possible collision channels.

When we want to compare the model with experimental data, such data are available only for hadron-nucleus collisions, collisions between light nuclei ($\alpha\alpha$) and for cosmic ray events. Some comparisons are shown in Figs 12–14, and we note a good agreement with the experiments.

For heavier nuclei there is a hope for a phase transition or other collective phenomena. The present model is based on "conventional colour dynamics", but we feel that it is very valuable to have such a conventional model to compare with when searching for new phenomena. Relevant quantities for the formation of a quark-gluon plasma are e.g. the baryon

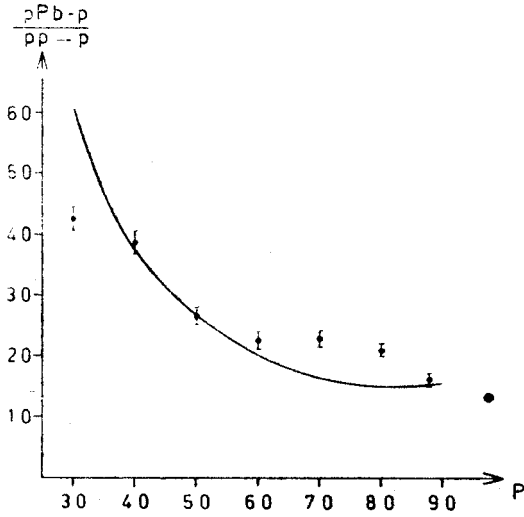


Fig. 12. The ratio between inclusive cross-sections for $p + \text{Pb} \rightarrow p$ and $pp \rightarrow p$ for $p_{\perp} = 0.3 \text{ GeV}/c$ and different momenta. The beam energy is 100 GeV. The line is the model predictions and the data are from [20]

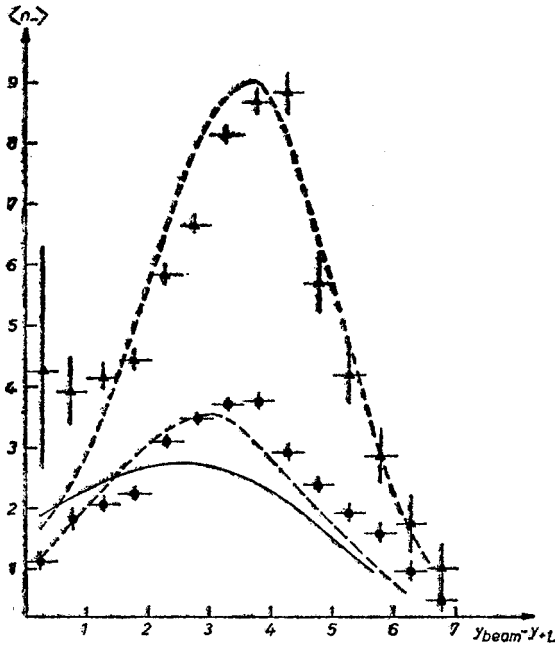


Fig. 13. Correlation between average negative multiplicity and the stopping of the positive charge in pp (●) and pXe (▲) collisions at 200 GeV/c. y_{+L} is the rapidity of the leading positively charged particle (assuming the kinematics of a pion). The dashed lines are the model predictions and the full line is the result from the old one-string model. The data are from Ref. [21]

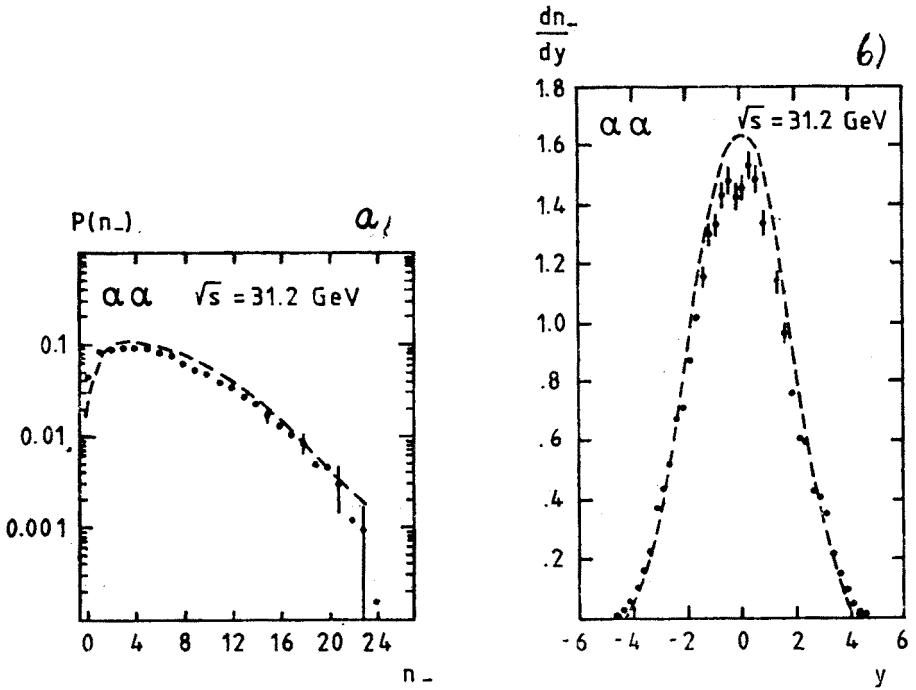


Fig. 14. Multiplicity (a) and rapidity (b) distributions for negative particles in $\alpha\alpha$ interactions at $\sqrt{s} = 31.2$ GeV. The curves are model calculations and the data are from Ref. [22]

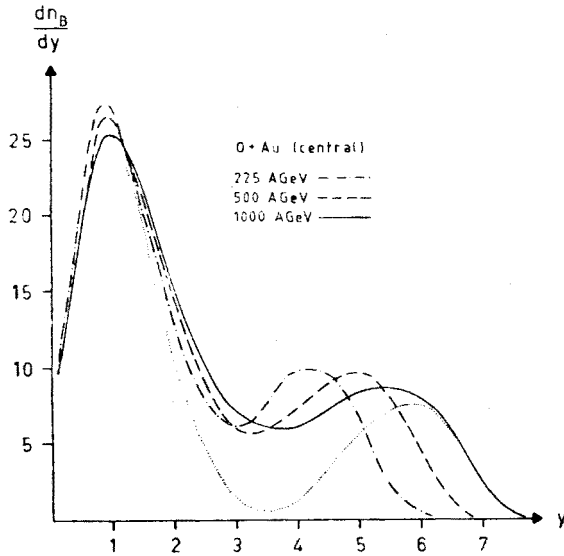


Fig. 15. The rapidity distribution of baryons ($\frac{dn_B}{dy}$) for "central" $0+Au$ events at different incident energies. The dotted line shows the distribution of baryon number, i.e. $\frac{dn_B}{dy} - \frac{dn_{anti-B}}{dy}$, at 1000 AGeV. Here the density in the central region is almost zero

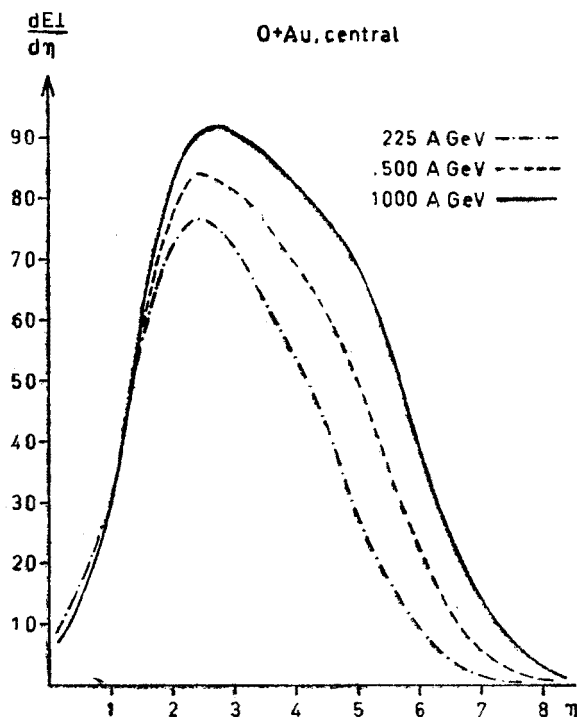


Fig. 16. The transverse energy distribution in pseudo-rapidity ($dE_{\perp}/d\eta$) for "central" O + Au events at different incident energies

number density, dB/dy , and the transverse energy density, dE_{\perp}/dy . The predictions for O + Au central collisions are shown in Figs 15, 16. We note that in the model there is a rather low "stopping power". The nucleus is rather transparent to the baryon number (cf. Figs 12 and 15) and the central energy density does not grow much with beam energy (Fig. 16).

It is also interesting to compare the model with the very high energy cosmic ray results. In Fig. 17 we show the multiplicity density for the highest energy JACEE event [23] together with an event generated by the Monte Carlo program for Si + Ag at 4A TeV. In this case there is in the centre of phase space just below 50 strings (corresponding to one or a few strings per fm² if we take a literal translation to a coordinate space picture). We note a rather large similarity between the observed and the generated event (the similarity would be increased if the real energy in the JACEE event is somewhat larger than the estimated 4A TeV). In particular we note that the very large fluctuations between different rapidity bins are well reproduced.

Summary

We have developed a model for hadron-hadron, hadron-nucleus and nucleus-nucleus collisions, based on the assumption that the colour field behaves like a vortex line in a type II superconductor.

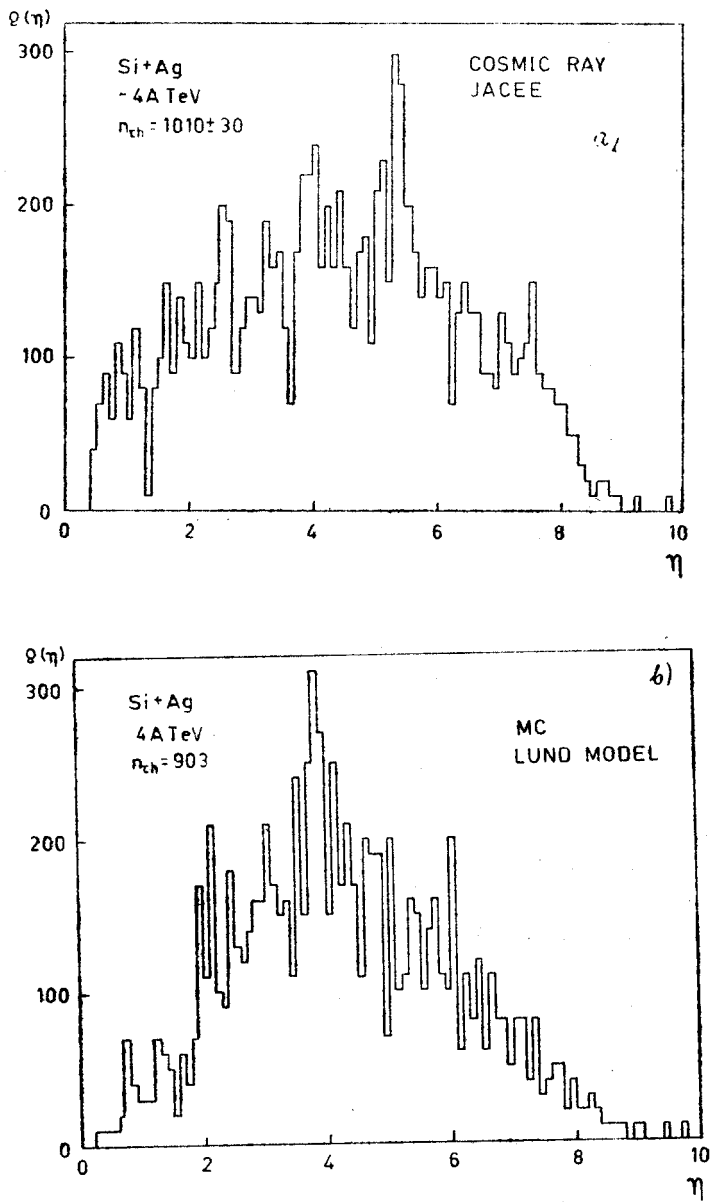


Fig. 17. The multiplicity distribution in pseudorapidity of a) the JACEE cosmic ray event Si+Ag with energy around 4A TeV [23] together with b) a model event

The model is infrared stable.
It works well for hh, hA and light nucleus collisions up to the top ISR energies.
When looking for new phenomena it is valuable to have a conventional model to compare with. (A Monte Carlo generation program is available.)
Further developments include the incorporation of hard parton-parton scatterings.

This can be done in an infrared stable way, and it is necessary in order to continue into the collider energy region.

Possible coherence phenomena could also be incorporated in the model, e.g. interactions between the strings and the formation of "ropes" [24].

REFERENCES

- [1] B. Andersson, G. Gustafson, G. Ingelman, T. Sjöstrand, *Phys. Rep.* **97**, 31 (1983).
- [2] B. Andersson, G. Gustafson, B. Nilsson-Almqvist, *Nucl. Phys.* **B281**, 289 (1987).
- [3] B. Nilsson-Almqvist, E. Stenlund, *Comput. Phys. Commun.* **43**, 387 (1987).
- [4] B. Andersson, G. Gustafson, B. Söderberg, *Z. Phys.* **C20**, 317 (1983).
- [5] B. Andersson, G. Gustafson, *Z. Phys.* **C3**, 22 (1980).
- [6] JADE Collaboration, W. Bartel et al., *Phys. Lett.* **101B**, 129 (1981); *Z. Phys.* **C21**, 37 (1983); TPC Collaboration, H. Aihara et al., *Z. Phys.* **C28**, 31 (1985); TASSO Collaboration, M. Althoff et al., *Z. Phys.* **C29**, 29 (1985).
- [7] I. Montvay, *Phys. Lett.* **84B**, 331 (1979).
- [8] C. Peterson, *Phys. Rev.* **34**, 1631 (1986).
- [9] A. Mueller, *Phys. Lett.* **104B**, 161 (1981); A. Bassetto, M. Ciafaloni, G. Marchesini, A. Mueller, *Nucl. Phys.* **B207**, 189 (1982); G. Marchesini, B. Webber, *Nucl. Phys.* **B238**, 1 (1984); B. Webber, *Nucl. Phys.* **B238**, 492 (1984); Ya. I. Azimov, Yu. L. Dokshitzer, V. A. Khoze, S. I. Troyan, *Coherence effects in QCD jets*, Leningrad preprint 1051 (1985).
- [10] JADE Collaboration, W. Bartel et al., *Z. Phys.* **C25**, 231 (1984).
- [11] B. Andersson, G. Gustafson, T. Sjöstrand, *Phys. Scr.* **32**, 574 (1985).
- [12] B. Andersson, G. Gustafson, B. Söderberg, *Nucl. Phys.* **B264**, 29 (1986).
- [13] B. Andersson, G. Gustafson, C. Peterson, *Phys. Lett.* **69B**, 221 (1977); **71B**, 337 (1977); B. Andersson, G. Gustafson, I. Holgersson, O. Månsson, *Nucl. Phys.* **B178**, 242 (1981).
- [14] T. Sjöstrand, *Multiple parton-parton interactions in hadronic events*, FERMILAB-Pub-85/119-T, and private communication.
- [15] A. Capella, U. Sukhatme, C. I. Tan, J. Tran Thanh Van, *Phys. Lett.* **81B**, 68 (1979); A. Capella, U. Sukhatme, J. Tran Thanh Van, *Z. Phys.* **C3**, 329 (1980); G. Cohen-Tannoudji, A. El-Hassouni, J. Kalinowski, O. Napoly, R. Peschanski, *Phys. Rev.* **D21**, 2699 (1980); P. Aurenche, F. W. Bopp, J. Ranft, *Z. Phys.* **C23**, 67 (1984); A. B. Kaidalov, *Phys. Lett.* **116B**, 459 (1982); X. Artru, G. Mennessier, *Nucl. Phys.* **B70**, 93 (1974).
- [16] D. Aston et al., *Nucl. Phys.* **B166**, 1 (1980); D. Bernard et al., *Phys. Lett.* **166B**, 459 (1986); A. M. Smith et al., *Phys. Lett.* **163B**, 267 (1985).
- [17] A. Breakstone et al., *Phys. Rev.* **D30**, 528 (1984).
- [18] A. Breakstone et al., *Phys. Lett.* **D132**, 458 (1983).
- [19] J. Whitmore et al., *Phys. Rev.* **D16**, 3137 (1977).
- [20] D. S. Barton et al., *Phys. Rev.* **D27**, 2580 (1983).
- [21] NA5 Collaboration, private communication.
- [22] W. Bell et al., *Phys. Lett.* **128B**, 349 (1983); *Z. Phys.* **C27**, 191 (1985).
- [23] T. H. Burnett et al., *Phys. Rev. Lett.* **50**, 2062 (1983).
- [24] T. S. Biro, H. B. Nielsen, J. Knoll, *Nucl. Phys.* **B245**, 449 (1984).